Supplementary Information

Collision-Induced Dissociation Mass Spectra of Na^+-Tagged Aldohexoses Simulated from First-Principles Calculations

Hai Thi Huynh[a], Jer-Lai Kuo[b,c,d,e], Cheng-chau Chiu[f,g,h*]

a. Department of Physics, Ho Chi Minh City University of Technology and Education, 700000 Ho Chi Minh City, Vietnam
b. Institute of Atomic and Molecular Sciences, Academia Sinica, Taipei, 10617, Taiwan
c. Molecular Science and Technology Program, Taiwan International Graduate Program, Academia Sinica, Taipei, 11529, Taiwan
d. International Graduate Program of Molecular Science and Technology (NTU-MST), National Taiwan University, Taipei 10617, Taiwan
e. Department of Chemistry, National Tsing Hua University, Hsinchu 30013, Taiwan
f. Department of Chemistry, National Sun Yat-sen University, Kaohsiung 80424, Taiwan
g. Green Hydrogen Research Center, National Sun Yat-sen University, Kaohsiung 80424, Taiwan
h. Center for Theoretical and Computational Physics, National Sun Yat-sen University, Kaohsiung 80424, Taiwan

*Corresponding author's email: ccchiu@mail.nsysu.edu.tw

SI. Transition state search

The majority of the transition state (TS) structures for the dehydration and ring-opening of cyclic aldohexoses at MP2/6-311+G(d,p) level were taken from a previous work, which explored the relevant conformational space by pre-optimizing the TS structures using semi-empirical methods.[S1] Recently, a neural network potential for Na^+-tagged saccharides has been developed and used for a more thorough search for TSs to ensure that no low-lying TSs for the cyclic aldohexoses have been missed.[S2] We have taken the low-lying TS from Ref [S2] and reoptimized them at MP2/6-311+G(d,p) level. An overview of the energies of the old and the newly found TS structures is given in **Table S1**.

The MP2 level TSs for the reactions of linear glucose and linear mannose, as well as of their isomers fructose and α/β-glutose, have been reported in our previous work on the CID-MS of fructose.[S3] Thus, for the current study, we merely lack the TSs for linear galactose and tagatose, which have now been searched using the same approach as in our previous study.[S3] For the sake of completeness of the documentation, the strategy is briefly outlined in the following. For dehydration TSs, we started with generating initial guess geometries from the optimized minima geometries. Here, any O atom of an OH group that is within 3 Å from the Na^+-cation was considered a potential proton donor. Then, as an O-O distance of 3 Å or less could be seen as an indicator of the presence of a hydrogen bond, any O atom that is within 3 Å of the proton donor O is considered a potential proton acceptor for the dehydration reaction. To generate an initial guess geometry, the proton of the proton donor group is moved towards the proton acceptor O, so the distance between the proton and the acceptor O atom is between 1.0 and 1.2 Å. In addition, the C-O bond to the proton acceptor O will be elongated to 1.8~2.1 Å. These parameters were chosen based on our previous experience in the TS search for different monosaccharides.[S3, S4] The obtained TS initial guesses are then pre-optimized at the PM6 level and then at B3LYP/6-311+G(d,p) level. Finally, the low-lying TSs are reoptimized at MP2/6-311+G(d,p) level of theory.

For C-C bond cleavage of linear galactose and tagatose, there is also a proton transfer step involved. While the proton acceptor is the carbonyl O, the proton donor is the OH group in β-position. The TS initial guesses here were generated by taking a suitable minimum geometry and shortening the distance between the transferring proton and the proton acceptor O to 1.1~1.2 Å while elongating the C-C bond being broken to 1.9~2.1 Å. A proton moves from the OH group at

O1 to the neighboring carbonyl group in the isomerization from linear galactose to tagatose. Also here, we have started from a suitable, (that means, the proton at O2 and the carbonyl O have a distance of less than 2.9 Å) optimized minimum structure of galactose and distorted the structure. In particular, the distance between the moving proton at O2 and the carbonyl O is changed to 1.2 Å, while the H atom in α-position is moved closer to the carbonyl C, displaying a distance of 1.1 Å. Due to the smaller number of TS initial guesses, the TS structures for isomerization and C-C bond breaking have been directly pre-optimized at B3LYP/6-311+G(d,p) before finally optimizing at MP2/6-311+G(d,p) level.

Table S1. The lowest dehydration and ring-opening barriers at MP2/6-311+G(d,p) level associated with the TSs found in our previous work [S1] (old) compared to the lowest barriers associated with the newly found TS structures. All barriers in kJ/mol.

	dehyd		ro	
	old	new	old	new
α-Glc	**200**	209	**182**	185
β-Glc	**214**	216	**178**	178
α-Gal	**196**	205	**189**	189
β-Gal	**211**	220	**172**	186
α-Man	**241**	247	**211**	214
β-Man	210	**205**	**185**	191

SII. Kinetic modeling

SII.1 Rate equations

The equations in the following sub-sections describe the kinetics of the studied systems. For all simulations, common boundary conditions are used. The boundary conditions state that at t = 0, the concentration of parent ions, i.e., one of the cyclic aldohexoses, is one, while all other species have a concentration of zero. In addition, it is required that the sum of changes in the concentration of all species at any time is always equal to one.

SII.1.1 Glucose

The full reaction network is described by the following set of differential equations:

$$\frac{d[dehyd]}{dt} = k_{1\alpha/\beta-Glc}[\alpha/\beta - Glc] + k_{1lGlc}[lGlc] + k_{1lFru}[lFru] + k_{1lMan}[lMan] + k_{1l\alpha Glut}[l\alpha Glut] + k_{1l\beta Glut}[l\beta Glut] \quad \text{(S2.1)}$$

$$\frac{d[desodiation]}{dt} = k_{3\alpha/\beta-Glc}[\alpha/\beta - Glc] + k_{3lGlc}[lGlc] + k_{3lFru}[lFru] + k_{3lMan}[lMan] + k_{3l\alpha Glut}[l\alpha Glut] + k_{3l\beta Glut}[l\beta Glut] \quad \text{(S2.2)}$$

$$\frac{d[m/z\ 113]}{dt} = k_{2lFru}[lFru] \quad \text{(S2.3)}$$

$$\frac{d[m/z\ 143]}{dt} = k_{2lGlc}[lGlc] + k_{2lMan}[lMan] + k_{2l\alpha Glut}[l\alpha Glut] + k_{2l\beta Glut}[l\beta Glut] \quad \text{(S2.4)}$$

$$\frac{d[m/z\ 83]}{dt} = k_{4l\alpha Glut}[l\alpha Glut] + k_{4l\beta Glut}[l\beta Glut] \quad \text{(S2.5)}$$

$$\frac{d[\alpha/\beta - Glc]}{dt} = -(k_{1\alpha/\beta-Glc} + k_{2\alpha/\beta-Glc} + k_{3\alpha/\beta-Glc})[\alpha/\beta - Glc] \quad \text{(S2.6)}$$

$$\frac{d[lGlc]}{dt} = k_{2\alpha/\beta-Glc}[\alpha/\beta - Glc] + k_{4lFru}[lFru] - (k_{1lGlc} + k_{2lGlc} + k_{3lGlc} + k_{4lGlc})[lGlc] \quad \text{(S2.7)}$$

$$\frac{d[lFru]}{dt} = k_{4lGlc}[lGlc] - (k_{1lFru} + k_{2lFru} + k_{3lFru} + k_{4lFru} + k_{5lFru} + k_{6lFru} + k_{7lFru})[lFru] \quad \text{(S2.8)}$$

$$\frac{d[lMan]}{dt} = k_{7lFru}[lFru] - (k_{1lMan} + k_{2lMan} + k_{3lMan} + k_{7lMan})[lMan] \quad \text{(S2.9)}$$

$$\frac{d[l\alpha Glut]}{dt} = k_{5lFru}[lFru] - (k_{1l\alpha Glut} + k_{2l\alpha Glut} + k_{3l\alpha Glut} + k_{4l\alpha Glut} + k_{5l\alpha Glut})[l\alpha Glut] \quad \text{(S2.10)}$$

$$\frac{d[l\beta Glut]}{dt} = k_{6lFru}[lFru] - (k_{1l\beta Glut} + k_{2l\beta Glut} + k_{3l\beta Glut} + k_{4l\beta Glut} + k_{6l\beta Glut})[l\beta Glut] \quad \text{(S2.11)}$$

In the partial reaction network, the differential equations simplify to:

$$\frac{d[dehyd]}{dt} = k_{1\alpha/\beta\,-\,Glc}[\alpha/\beta - Glc] + k_{1lGlc}[lGlc] + k_{1lFru}[lFru] \quad \text{(S2.12)}$$

$$\frac{d[desodiation]}{dt} = k_{3\alpha/\beta\,-\,Glc}[\alpha/\beta - Glc] + k_{3lGlc}[lGlc] + k_{3lFru}[lFru] \quad \text{(S2.13)}$$

$$\frac{d[m/z\ 113]}{dt} = k_{2lFru}[lFru] \quad \text{(S2.14)}$$

$$\frac{d[m/z\ 143]}{dt} = k_{2lGlc}[lGlc] \quad \text{(S2.15)}$$

$$\frac{d[\alpha/\beta - Glc]}{dt} = -(k_{1\alpha/\beta\,-\,Glc} + k_{2\alpha/\beta\,-\,Glc} + k_{3\alpha/\beta\,-\,Glc})[\alpha/\beta - Glc] \quad \text{(S2.16)}$$

$$\frac{d[lGlc]}{dt} = k_{2\alpha/\beta\,-\,Glc}[\alpha/\beta - Glc] + k_{4lFru}[lFru] - (k_{1lGlc} + k_{2lGlc} + k_{3lGlc} + k_{4lGlc})[lGlc] \quad \text{(S2.17)}$$

$$\frac{d[lFru]}{dt} = k_{4lGlc}[lGlc] - (k_{1lFru} + k_{2lFru} + k_{3lFru} + k_{4lFru})[lFru] \quad \text{(S2.18)}$$

SII.1.2 Mannose

The full reaction network is described by the following set of differential equations:

$$\frac{d[dehyd]}{dt} = k_{1\alpha/\beta-Man}[\alpha/\beta - Man] + k_{1lMan}[lMan] + k_{1lFru}[lFru] + k_{1lGlc}[lGlc] + k_{1l\alpha Glut}[l\alpha Glut] + k_{1l\beta Glut}[l\beta Glut] \quad \text{(S2.19)}$$

$$\frac{d[desodiation]}{dt} = k_{3\alpha/\beta-Man}[\alpha/\beta - Man] + k_{3lGlc}[lGlc] + k_{3lFru}[lFru] + k_{3lMan}[lMan] + k_{3l\alpha Glut}[l\alpha Glut] + k_{3l\beta Glut}[l\beta Glut] \quad \text{(S2.20)}$$

$$\frac{d[m/z\ 113]}{dt} = k_{2lFru}[lFru] \quad \text{(S2.21)}$$

$$\frac{d[m/z\ 143]}{dt} = k_{2lGlc}[lGlc] + k_{2lMan}[lMan] + k_{2l\alpha Glut}[l\alpha Glut] + k_{2l\beta Glut}[l\beta Glut] \quad \text{(S2.22)}$$

$$\frac{d[m/z\ 83]}{dt} = k_{4l\alpha Glut}[l\alpha Glut] + k_{4l\beta Glut}[l\beta Glut] \quad \text{(S2.23)}$$

$$\frac{d[\alpha/\beta - Man]}{dt} = -(k_{1\alpha/\beta-Man} + k_{2\alpha/\beta-Man} + k_{3\alpha/\beta-Man})[\alpha/\beta - Man] \quad \text{(S2.24)}$$

$$\frac{d[lGlc]}{dt} = k_{7lFru}[lFru] - (k_{1lGlc} + k_{2lGlc} + k_{3lGlc} + k_{7lGlc})[lGlc] \quad \text{(S2.25)}$$

$$\frac{d[lFru]}{dt} = k_{4lMan}[lMan] - (k_{1lFru} + k_{2lFru} + k_{3lFru} + k_{4lFru} + k_{5lFru} + k_{6lFru} + k_{7lFru})[lFru] \quad \text{(S2.26)}$$

$$\frac{d[lMan]}{dt} = k_{2\alpha/\beta-Man}[\alpha/\beta - Man] + k_{4lFru}[lFru] - (k_{1lMan} + k_{2lMan} + k_{3lMan} + k_{4lMan})[lMan] \quad \text{(S2.27)}$$

$$\frac{d[l\alpha Glut]}{dt} = k_{5lFru}[lFru] - (k_{1l\alpha Glut} + k_{2l\alpha Glut} + k_{3l\alpha Glut} + k_{4l\alpha Glut} + k_{5l\alpha Glut})[l\alpha Glut] \quad \text{(S2.28)}$$

$$\frac{d[l\beta Glut]}{dt} = k_{6lFru}[lFru] - (k_{1l\beta Glut} + k_{2l\beta Glut} + k_{3l\beta Glut} + k_{4l\beta Glut} + k_{6l\beta Glut})[l\beta Glut] \quad \text{(S2.29)}$$

In the partial reaction network, the differential equations simplify to:

$$\frac{d[dehyd]}{dt} = k_{1\alpha/\beta\,-\,Man}[\alpha/\beta - Man] + k_{1lMan}[lMan] + k_{1lFru}[lFru] \quad \text{(S2.30)}$$

$$\frac{d[desodiation]}{dt} = k_{3\alpha/\beta\,-\,Glc}[\alpha/\beta - Man] + k_{3lFru}[lFru] + k_{3lMan}[lMan] \quad \text{(S2.31)}$$

$$\frac{d[m/z\ 113]}{dt} = k_{2lFru}[lFru] \quad \text{(S2.32)}$$

$$\frac{d[m/z\ 143]}{dt} = k_{2lGlc}[lGlc] + k_{2lMan}[lMan] \quad \text{(S2.33)}$$

$$\frac{d[\alpha/\beta - Man]}{dt} = -(k_{1\alpha/\beta\,-\,Man} + k_{2\alpha/\beta\,-\,Man} + k_{3\alpha/\beta\,-\,Man})[\alpha/\beta - Man] \quad \text{(S2.34)}$$

$$\frac{d[lFru]}{dt} = k_{4lMan}[lMan] - (k_{1lFru} + k_{2lFru} + k_{3lFru} + k_{4lFru})[lFru] \quad \text{(S2.35)}$$

$$\frac{d[lMan]}{dt} = k_{2\alpha/\beta\,-\,Man}[\alpha/\beta - Man] + k_{4lFru}[lFru] - (k_{1lMan} + k_{2lMan} + k_{3lMan} + k_{4lMan})[lMan] \quad \text{(S2.36)}$$

SII.1.3 Galactose

For galactose, only a partial reaction network has been considered, which is given by the following differential equations:

$$\frac{d[\alpha/\beta - Gal]}{dt} = (k_{1\alpha/\beta\,-\,Gal} + k_{2\alpha/\beta\,-\,Gal} + k_{3\alpha/\beta\,-\,Gal})[\alpha/\beta - Gal] \quad \text{(S2.37)}$$

$$\frac{d[dehyd]}{dt} = k_{1\alpha/\beta\,-\,Gal}[\alpha/\beta - Gal] + k_{1lGal}[lGal] + k_{1lTag}[lTag] \quad \text{(S2.38)}$$

$$\frac{d[m/z\ 143]}{dt} = k_{2lGal}[lGal] \quad \text{(S2.39)}$$

$$\frac{d[m/z\ 113]}{dt} = k_{2lTag}[lTag] \tag{S2.40}$$

$$\frac{d[desodiation]}{dt} = k_{3\alpha/\beta\ -\ Gal}[\beta - Gal] + k_{3lGal}[lGal] + k_{3lTag}[lTag] \tag{S2.41}$$

$$\frac{d[lGal]}{dt} = k_{2\alpha/\beta\ -\ Gal}[\alpha/\beta - Gal] - \left(k_{1lGal} + k_{2lGal} + k_{3lGal}\right)[lGal] \tag{S2.42}$$

$$\frac{d[lTag]}{dt} = k_{4lGal}[lGal] - \left(k_{1lTag} + k_{2lTag} + k_{3lTag} + k_{4lTag}\right)[lTag] \tag{S2.43}$$

SII.2 Sensitivity test

We have conducted a sensitivity test at the example of the kinetic model for the full reaction network of α-Glc, as shown in Figure 2a of the main text. Here, we have taken all reaction channels with well-defined TSs and systematically increased the energy of the lowest-lying TS for a reaction channel by 2 kJ/mol. Using the changed TS energy, we have re-run the kinetic simulation with the obtained signal intensities denoted I'. In contrast, the signal intensities obtained with the original TS energies are referred to as I. To estimate how the signal intensities change when the reaction barrier E_a changes, we have used the approximation

$$\frac{dI}{dE_a} \approx \frac{I' - I}{2\ kJ/mol} \tag{S2.44}$$

By varying the barriers for one reaction at a time, we have estimated the impact of each reaction on the simulated signal intensities. Note that when dealing with reversible reactions, we have increased the barriers for both the reactions in forward and backward directions at the same time. To get a rough idea of the overall impact on the signal intensities, we have also used $\sqrt{[\Sigma(\mathrm{d}I/\mathrm{d}E_a)^2]}$ as a measure. Here, we formally treat the changes in the intensity of the different signals as the entries of an n-dimensional vector. The larger the (Euclidian) norm of the vector, the more pronounced the changes in the signal intensities. The results of the sensitivity test are shown in Table S2.

Table S2. Results of the sensitivity test for the final, relative product concentrations, which directly correspond to the simulated signal intensities. dI/dE_a denotes the change in the simulated signal intensity upon varying the energy of the lowest-lying TS for a reaction channel. All values in units of mol/kJ.

reaction	dI/dE_a				$\sqrt{[\Sigma(dI/dE_a)^2]}$	
	m/z 185	143	113	83	all signals	only cross-ring[a]
1α-Glc	**-2.05×10^{-2}**	**1.92×10^{-2}**	1.30×10^{-3}	2.45×10^{-5}	**2.81×10^{-2}**	**1.92×10^{-2}**
2α-Glc	**1.42×10^{-2}**	**-1.33×10^{-2}**	-9.11×10^{-4}	-1.70×10^{-5}	**1.95×10^{-2}**	**1.33×10^{-2}**
4lαGlut	-4.93×10^{-8}	-1.63×10^{-8}	1.11×10^{-7}	-3.09×10^{-8}	1.26×10^{-7}	1.16×10^{-7}
2lαGlut	5.54×10^{-6}	-2.90×10^{-5}	1.92×10^{-5}	4.60×10^{-6}	3.58×10^{-5}	3.54×10^{-5}
1lαGlut	-5.26×10^{-12}	1.58×10^{-11}	3.13×10^{-12}	4.37×10^{-13}	1.69×10^{-11}	1.61×10^{-11}
4lβGlut	1.14×10^{-6}	1.13×10^{-5}	4.05×10^{-6}	-1.60×10^{-5}	2.04×10^{-5}	2.04×10^{-5}
2lβGlut	4.69×10^{-7}	-2.68×10^{-6}	2.05×10^{-6}	1.59×10^{-7}	3.41×10^{-6}	3.38×10^{-6}
5lFru/5lαGlut	-8.39×10^{-8}	-1.37×10^{-7}	1.70×10^{-7}	-2.02×10^{-8}	2.35×10^{-7}	2.20×10^{-7}
6lFru/6lβGlut	4.97×10^{-10}	-2.75×10^{-8}	7.05×10^{-8}	7.34×10^{-9}	7.61×10^{-8}	7.61×10^{-8}
4lFru/4lGlc	1.13×10^{-5}	-8.59×10^{-5}	7.32×10^{-5}	1.42×10^{-6}	1.13×10^{-4}	1.13×10^{-4}
7lFru/7lMan	-3.37×10^{-6}	2.77×10^{-5}	-2.39×10^{-5}	-4.69×10^{-7}	3.67×10^{-5}	3.66×10^{-5}
2lFru	4.41×10^{-5}	3.19×10^{-4}	-3.70×10^{-4}	5.13×10^{-6}	4.89×10^{-4}	4.87×10^{-4}
1lFru	-4.80×10^{-10}	3.46×10^{-10}	1.32×10^{-10}	1.12×10^{-11}	6.03×10^{-10}	3.70×10^{-10}
2lGlc	-1.70×10^{-7}	-1.90×10^{-7}	3.49×10^{-7}	-8.40×10^{-9}	4.33×10^{-7}	3.99×10^{-7}
1lGlc	1.32×10^{-12}	9.71×10^{-12}	2.71×10^{-12}	3.37×10^{-13}	1.02×10^{-11}	1.01×10^{-11}
2lMan	1.61×10^{-5}	-7.90×10^{-5}	6.19×10^{-5}	1.16×10^{-6}	1.02×10^{-4}	1.01×10^{-4}
1lMan	-4.98×10^{-8}	-3.08×10^{-10}	1.14×10^{-7}	3.89×10^{-9}	1.25×10^{-7}	1.14×10^{-7}

[a]only signals at *m/z* 113, 143, and 83

SII.3 Influence of *c* on the final product concentration

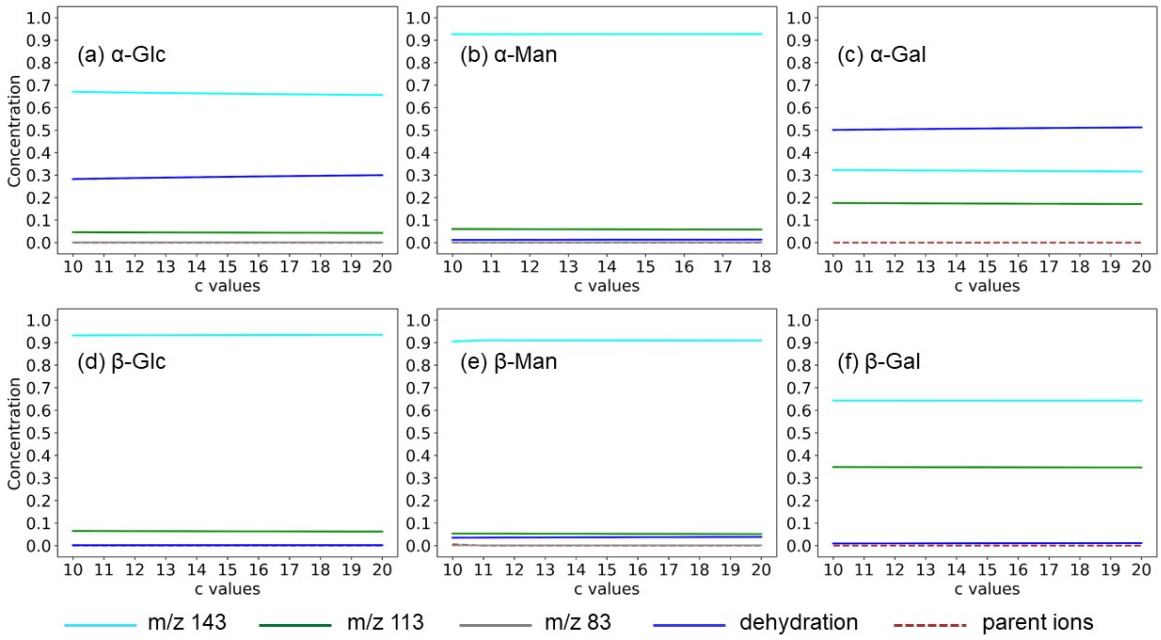

Figure S1. Simulated final, relative concentrations for the products obtained from the dissociation of the considered aldohexoses as a function of the applied value of *c*.

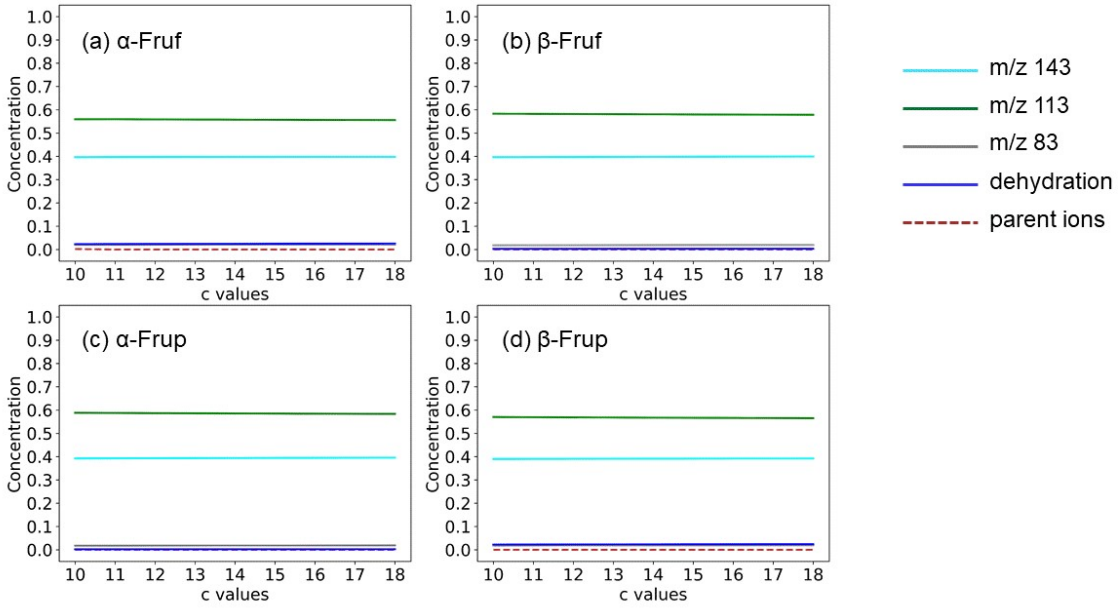

Figure S2. Simulated final, relative concentrations for the products obtained from the dissociation of fructose as a function of the applied value of *c*. The energetics for the kinetic simulations and the reaction network are taken from Ref [S3].

SIII. Reaction barriers

Table S3. Summary of the lowest reaction barriers at MP2/6-311+G(d,p) level for the different dissociation reaction channels of the considered monosaccharides. All values in units of kJ/mol.

	α anomer		β anomer		linear sugars[a]		
	dehyd	ro	dehyd	ro	dehyd	C-C scission	isomerization
Glc	200	182	214	178	256	153 (C2-C3)	166 (lGlc → lFru)
Man	241	211	205	185	224	157 (C2-C3)	166 (lMan → lFru)
Gal	196	189	211	172	253	171 (C2-C3)	168 (lGal → lTag)
Tag					229	148 (C3-C4)	169 (lTag → lGal)
Fru					237	158 (C3-C4)	176 (lFru → lMan)
							177 (lFru → lGlc)
							173 (lFru → lαGlut)
							168 (lFru → lβGlut)
αGlut					240	167 (C4-C5)	176 (lαGlut → lFru)
βGlut					250	190 (C4-C5)	182 (lβGlut → lFru)

[a]Data for lGlc, lMan, lFru, lαGlut, and lβGlut were taken from Ref [S3]. Data for lGal and lTag calculated in this work.

SIV. Dehydration mechanism for cyclic aldohexoses

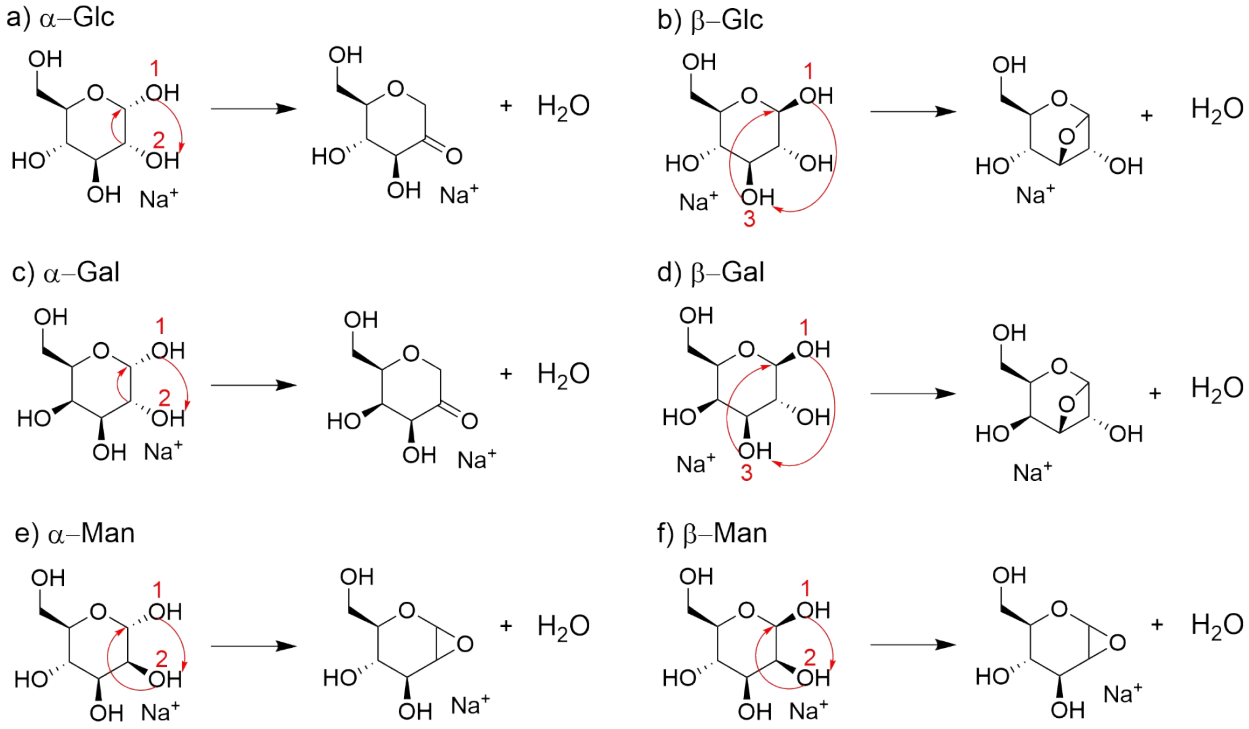

Figure S3. Dehydration mechanism for the considered cyclic aldohexoses.

SV. Simulated MS signal intensities

Table S4. The simulated, final signal intensities as obtained from the relative product concentrations for the different dissociation channels. Results as obtained with the full reaction network as shown in Figure 2 of the main text.

	Parent ions	dehyd	*m/z* 143	*m/z* 113	*m/z* 83
α-Glc	0.0	2.85×10^{-1}	6.69×10^{-1}	4.56×10^{-2}	8.55×10^{-4}
β-Glc	0.0	1.59×10^{-3}	9.33×10^{-1}	6.45×10^{-2}	1.20×10^{-3}
α-Man	0.0	1.23×10^{-2}	9.27×10^{-1}	5.96×10^{-2}	1.19×10^{-3}
β-Man	0.0	3.64×10^{-2}	9.10×10^{-1}	5.25×10^{-2}	1.19×10^{-3}

Table S5. The simulated, final signal intensities as obtained from the relative product concentrations for the different dissociation channels. Results as obtained with the partial reaction network as shown in Figure 2 of the main text. The simulated signal intensity ratio in Table 1 and mass spectra in Figure 6 of the main text are obtained based on the results from this table.

	Parent ions	dehyd	m/z 143	m/z 113
α-Glc	0.0	8.29×10^{-1}	1.54×10^{-1}	1.64×10^{-2}
β-Glc	0.0	7.81×10^{-1}	2.14×10^{-1}	4.86×10^{-3}
α-Man	0.0	1.24×10^{-2}	8.97×10^{-1}	9.04×10^{-2}
β-Man	0.0	3.69×10^{-2}	8.85×10^{-1}	7.81×10^{-2}
α-Gal	0.0	5.04×10^{-1}	3.21×10^{-1}	1.75×10^{-1}
β-Gal	0.0	9.93×10^{-3}	6.42×10^{-1}	3.48×10^{-1}

References

[S1]. C.C. Chiu, C.K. Lin, J.L. Kuo, Improved agreement between experimental and computational results for collision-induced dissociation mass spectrometry of cation-tagged hexoses, Phys Chem Chem Phys 22 (2020) 6928-6941.

[S2]. P.K. Tsou, H.T. Huynh, H.T. Phan, J.L. Kuo, A self-adapting first-principles exploration on the dissociation mechanism in sodiated aldohexose pyranoses assisted with neural network potentials, Phys Chem Chem Phys 25 (2023) 3332-3342.

[S3]. H.T. Huynh, S.T. Tsai, P.J. Hsu, A. Biswas, H.T. Phan, J.L. Kuo, C.K. Ni, C.C. Chiu, Collision-induced dissociation of $Na(^{+})$-tagged ketohexoses: experimental and computational studies on fructose, Phys Chem Chem Phys 24 (2022) 20856-2086.

[S4] H.T. Huynh, H.T. Phan, P.J. Hsu, J.L. Chen, H.S. Nguan, S.T. Tsai, T. Roongcharoen, C.Y. Liew, C.K. Ni, J.L. Kuo, Collision-induced dissociation of sodiated glucose, galactose, and mannose, and the identification of anomeric configurations, Phys Chem Chem Phys 20 (2018) 19614-19624.